JSCE (Journal of System and Computer Engineering)
Vol.7, No.4, October 2026, pp. 519-531
ISSN (online): 2723-1240
DOI : https://doi.org/10.61628/jsce.v7i4.2962

Research Article Open Access (CC–BY-SA) ■

Early Detection of Potential Tip Burn and Frog Eye in Hydroponic Lettuce Based on Environmental Conditions Using Naive Bayes on ESP32

Fadhlan Muhammad 1,a,*; Wardi 2,b; Imran Taufik 1,c; Mashur Razak 1,d; Abdul Latief Arda 1,e; Supriadi Sahibu 1,f

1 Department of Computer Systems, Universitas Handayani Makassar, Makassar, Indonesia
2 Faculty of Engineering, Universitas Hasanuddin, Indonesia
a fadhlanmuhh@gmail.com; b wardi@unhas.ac.id; c imran_taufik@handayani.ac.id; d mashur_razak@yahoo.co.id; e abdullatief@handayani.ac.id; f supriadi@handayani.ac.id
** Corresponding author*

Abstract

*Lettuce (*Lactuca sativa *L.) is a high-value horticultural commodity susceptible to tip burn, a calcium deficiency disorder triggered by high temperature and low humidity, and frog eye, a fungal leaf spot caused by* Cercospora canescens *that thrives under low temperature and high humidity. Visual inspection detects both only after damage has occurred. This study developed an Internet of Things early detection system that classifies environmental risk conditions using Gaussian Naive Bayes embedded directly on an ESP32 microcontroller. The system integrates DHT22, pH, and TDS sensors and sends automatic Telegram notifications. Environmental data were collected for 31 days at a hydroponic farm in Makassar, yielding 1,005 valid records after preprocessing. The initial Gaussian Naive Bayes model, parameterized from simulated data, was deployed on the ESP32 as embedded machine learning, and its outputs served as labels for the field data. The simulation model achieved 95.56 percent accuracy on synthetic test samples, while a real-data model trained in Python with scikit-learn reproduced these labels with 94.03 percent agreement on 201 test samples, with a five-fold cross-validation agreement of 92.91 percent and a spread of only 0.12 percent across four validation methods; this is not an independent measure of detection accuracy. Field visual validation of the deployed model showed 52 percent agreement (13 of 25 alerts), indicating that the system is best suited as an early warning of conducive conditions rather than as a symptom diagnosis tool.*

Keywords*—Embedded Machine Learning, ESP32, Frog Eye, Naive Bayes, Tip Burn*

1. Introduction

Lettuce (*Lactuca sativa* L.) is a high-value horticultural commodity that is widely cultivated hydroponically. The growth and quality of hydroponic lettuce depend strongly on suitable air temperature and humidity, as well as on nutrient solution quality expressed as acidity (pH) and total dissolved solids (TDS) (Syaimah et al., 2025; Lestari et al., 2022). The success of cultivation in Nutrient Film Technique (NFT) and Deep Flow Technique (DFT) systems is also determined by the stability of these environmental parameters (Zahra et al., 2023); therefore, environmental factors are not merely supportive but decisive in whether plants grow optimally or suffer from disorders.

Two disorders that frequently reduce lettuce quality are tip burn and frog eye. Tip burn is a physiological disorder caused by calcium (Ca2+) deficiency in young leaf tissue, which occurs when calcium translocation cannot keep pace with leaf growth, particularly when transpiration is disrupted by unsuitable temperature and humidity (de Bang et al., 2021; Hamidon & Ahamed, 2022). Frog eye is a leaf spot disease caused by *Cercospora* fungi that develops under high humidity (To-Anun & Meeboon, 2011; Nguanhom et al., 2015); a study in Bali reported that this disease can cause significant yield losses in lettuce crops (Mirah et al., 2023; Supakitthanakorn et al., 2023). Although the plants can continue to grow, both disorders reduce the visual quality and market value of lettuce.

In practice, plant disorders are generally still detected through visual observation by farmers. This approach is subjective, depends on experience, and risks being too late because symptoms become visible only after tissue damage has occurred (Shafik et al., 2023). Image-based approaches using deep learning have detected tip burn with high accuracy (Hamidon & Ahamed, 2022; Qin et al., 2025; Dolatabadian et al., 2025), but they require cameras, controlled lighting, and substantial computing resources (Luo et al., 2024). Moreover, image-based approaches still operate only after symptoms appear. Approaches based on environmental data offer a lighter alternative with the potential to provide warnings before symptoms emerge (Valleggi & Stefanini, 2024; Mohyuddin et al., 2024).

The use of the Internet of Things (IoT) in hydroponic lettuce cultivation in Indonesia has been widely reported, including nutrient, pH, and temperature monitoring based on ESP32 and Blynk (Prasetyo et al., 2022), automatic pH and nutrient control (Wati & Sholihah, 2021), and temperature, pH, and water level monitoring based on ESP8266 (Prabowo et al., 2023; Tarigan et al., 2023). Similar applications have also been implemented in community empowerment programs, irrigation systems, and educational settings (Purwalaksana et al., 2024; Kurniawan & Putra, 2026; Riansyah et al., 2025). However, most of these systems stop at monitoring and automation without the ability to classify risk conditions. Meanwhile, the integration of machine learning into smart agriculture continues to grow (Ali et al., 2023; Gourshettiwar & Reddy, 2026), and the Naive Bayes algorithm has been used for disease prediction (Meshram et al., 2022), symptom-based rice disease diagnosis (Susanto et al., 2026), and irrigation automation (Saputra & Santiyasa, 2024). This algorithm was chosen because it is fast, efficient on small to medium-sized data, and computationally lightweight, making it suitable for microcontrollers. Nevertheless, these studies generally run the model on a server or web application, require manual symptom input, or do not specifically target tip burn and frog eye.

Based on this gap, this study aims to develop an early detection system for tip burn and frog eye risk in hydroponic lettuce based on environmental conditions, using Gaussian Naive Bayes implemented directly on the ESP32 and accompanied by automatic notifications via Telegram. The contributions of this study are: (1) an IoT system in which Gaussian Naive Bayes classification is computed locally on the ESP32 and linked to Telegram notifications, with its resource requirements measured on the device (Section 3.7); (2) an evaluation using 31 days of field data and four cross-validation methods, with an explicit analysis of the limitation that the labels originate from the initial model; and (3) field visual validation that quantifies the gap between risky environmental conditions and the symptoms actually visible on the plants. Unlike prior Naive Bayes applications in agriculture that run on servers, require manual symptom input, or do not target tip burn and frog eye, this study targets the environmental risk of both disorders with on-device inference.

2. Method

2.1 Study Site and Research Stages

The study was conducted at the Cocotani Hydroponic farm, Manggala District, Makassar City, in a 10 × 15 m greenhouse with 2,047 planting holes in an NFT system. The research stages comprised system design, hardware assembly and programming, sensor calibration, field data

collection, data preprocessing, model training and evaluation, model implementation on the ESP32, and functional testing and field visual validation.

2.2 System Architecture

The system architecture is shown in Figure 1. The main processing unit is an ESP32-S microcontroller (dual-core 240 MHz with 2.4 GHz Wi-Fi) connected to a DHT22 sensor for air temperature and relative humidity, a PH-4502C pH sensor for nutrient solution acidity, a TDS Meter V1.0 sensor for nutrient concentration, and a 0.96-inch OLED display for local output. Sensor data are transmitted via Wi-Fi to Blynk for real-time monitoring, to Google Sheets for logging, and to Telegram for notifications.

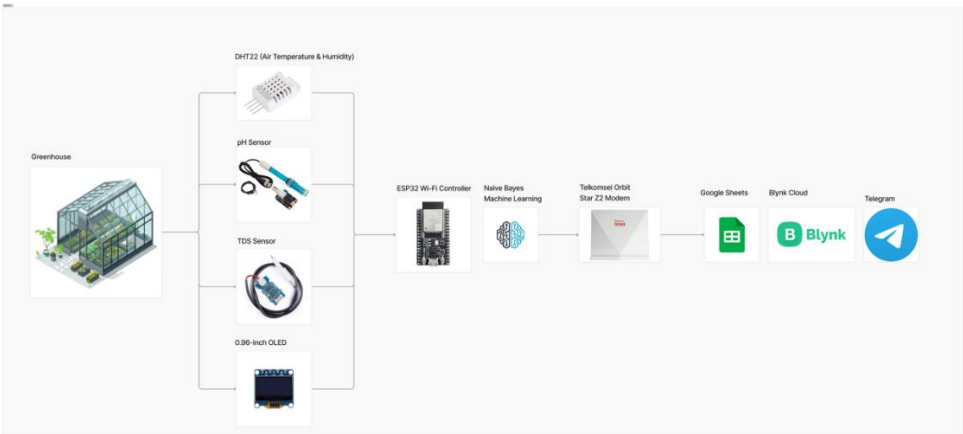


Figure 1. Architecture of the IoT-Based Early Detection System

The system workflow is shown in Figure 2. Sensors are read and classified every 10 seconds, Blynk data are updated every 10 minutes, and pH and TDS monitoring reports are sent and logged to Google Sheets every 30 minutes. Classification alerts are sent using an edge-triggered scheme, that is, only when a new risk condition is detected, when the status changes, when an abnormal condition persists for at least 6 hours (as a reminder), or when conditions return to normal (as a recovery notification). This scheme was chosen so that farmers do not receive repeated messages for the same condition.

2.3 Sensor Calibration

Calibration was performed before system operation by comparing the IoT sensor readings against reference instruments. The DHT22 sensor was compared with a digital thermometer and hygrometer, with tolerance limits of ±0.5 °C for temperature and ±5% RH for humidity according to the manufacturer's datasheet (AOSONG Electronics). The pH sensor was compared with a digital pH meter with a tolerance of ±0.2 pH (Flores-Iwasaki et al., 2025); its readings were stabilized by sorting 30 samples and averaging the middle 20, then converted using a linear calibration equation. The TDS sensor was compared with a digital TDS meter with a tolerance of ±10% of the reference value (Harjanto et al., 2026); its readings were temperature-compensated, converted using a polynomial equation, and then calibrated with a multiplication factor.

2.4 Data Collection and Preprocessing

Data were collected automatically every 30 minutes for 31 days, from 24 April to 25 May 2026, yielding 1,178 rows. Preprocessing removed 173 rows from periods when the DHT22 sensor was stuck at 26.1 °C and 97.9%. Anomalies in the pH (182 rows) and TDS (3 rows) readings were not removed because these two parameters were not used as classification features. The final clean dataset comprised 1,005 rows, which were split by stratified sampling at an 80:20 ratio into 804 training and 201 test samples.

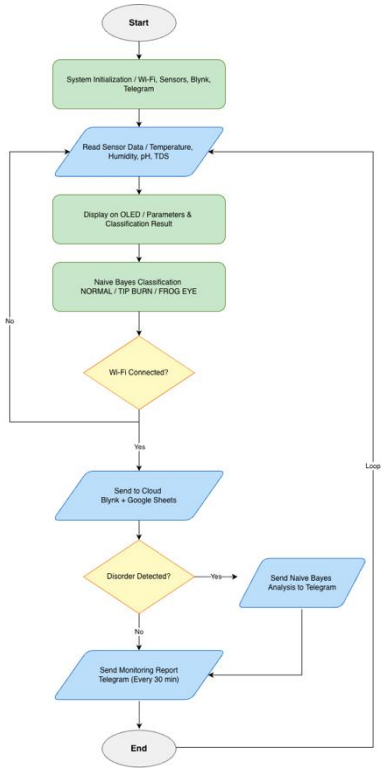


Figure 2. System Flowchart

During data collection, the ESP32 ran an initial Gaussian Naive Bayes model whose parameters were obtained by training on simulated data based on literature-derived conditions that trigger tip burn and frog eye (de Bang et al., 2021; Hamidon & Ahamed, 2022; Mirah et al., 2023), as summarized in Table 1. The label of each record was taken from the classification output of this initial model logged in Google Sheets. The labels were therefore not assigned by experts: they reflect the decision boundaries of the initial model, which was parameterized from simulated data (150 synthetic samples per class) rather than from independently verified plant conditions. A real-data model was later trained on these labels offline and was not deployed on the ESP32 in this study. The only agricultural criteria encoded in the labels are the literature-derived conditions in Table 1, which were not verified by expert diagnosis in this study. The pH and TDS parameters have the same optimal range for all three classes; therefore, both serve as nutrient solution quality monitoring parameters separate from the classification. The class distribution after preprocessing is shown in Table 2.

Table 1. Condition Parameters of the Classification Classes

Parameter	Unit	TIP_BURN	NORMAL	FROG_EYE
Air temperature	°C	30–45	23–33	15–26
Relative humidity	%	50–74	65–75	76–100
Solution pH	pH	5.5–6.5	5.5–6.5	5.5–6.5
Solution TDS	ppm	800–1200	800–1200	800–1200

Table 2. Class Distribution after Preprocessing

Class	Count	Percentage (%)	Dominant period
FROG_EYE	570	56.72	Night (18:00–08:00)
TIP_BURN	295	29.35	Daytime (09:00–17:00)
NORMAL	140	13.93	Morning and evening transitions
Total	1,005	100.00	–

2.5 Gaussian Naive Bayes

Naive Bayes is a probabilistic classification algorithm based on Bayes' theorem with the assumption of conditional independence between features (Meshram et al., 2022). The posterior probability of a class C given a feature vector x is expressed in Equation (1), where $P(x|C)$ is the likelihood, $P(C)$ is the prior, and $P(x)$ is the normalization constant.

$$P(C \mid \mathbf{x}) = \frac{P(\mathbf{x}|C)\,P(C)}{P(\mathbf{x})} \quad (1)$$

Because the temperature and humidity features are continuous, the likelihood of each feature is modeled using the Gaussian probability density function in Equation (2), where $\mu_{C,i}$ and $\sigma 2_{C,i}$ are the mean and variance of the i-th feature in class C, respectively.

$$P(x_i \mid C) = \frac{1}{\sqrt{2\pi\sigma_{C,i}^2}} \exp\left(-\frac{(x_i-\mu_{C,i})^2}{2\sigma_{C,i}^2}\right) \quad (2)$$

To avoid numerical underflow on the microcontroller, computations are performed in logarithmic form, and the class with the highest log-posterior value is selected as the classification result according to Equation (3), with $n = 2$ features.

$$\hat{C} = \underset{C}{\operatorname{argmax}}[\log P(C) + \textstyle\sum_{i=1}^{n} \log P(x_i \mid C)] \quad (3)$$

Before using field data, a simulation model was built as a baseline to verify that the three classes can be separated by Gaussian Naive Bayes. The simulation dataset consisted of 450 balanced synthetic samples (150 per class) generated from normal distributions around the parameter ranges in Table 1, which were then split into 360 training and 90 test samples. This simulation model served as the initial model on the ESP32 with balanced priors (0.3333 for each class). All training was performed using Python and the scikit-learn library.

2.6 Model and System Evaluation

Model performance was evaluated using accuracy, precision, recall, and F1-score computed from the confusion matrix according to Equations (4)–(7), where TP_k, FP_k, and FN_k are the true positives, false positives, and false negatives of class k, respectively, $K = 3$ classes, and N is the number of test samples. For the field data, the labels were generated by the initial model; therefore, accuracy, precision, recall, and F1-score denote agreement with these model-generated labels rather than performance against independently verified plant conditions.

$$\text{Accuracy} = \frac{\sum_{k=1}^{K} TP_k}{N} \times 100\% \quad (4)$$

$$\text{Precision}_k = \frac{TP_k}{TP_k+FP_k} \quad (5)$$

$$\text{Recall}_k = \frac{TP_k}{TP_k+FN_k} \quad (6)$$

$$F1_k = \frac{2\times\text{Precision}_k\times\text{Recall}_k}{\text{Precision}_k+\text{Recall}_k} \quad (7)$$

Model stability was assessed using four cross-validation methods on the training data, namely 3-fold, 5-fold, 10-fold, and Leave-One-Out (LOO). The IoT system was functionally tested against target intervals for sensor reading, classification, notification delivery, and data storage. In addition, visual validation was performed on 25 samples from 19 to 26 September 2026 by matching the system's classification results with direct observations of plant condition while the farmer was at the farm in the morning and afternoon.

2.7 Model Implementation on the ESP32 (Embedded Machine Learning)

The parameters of the trained initial model, namely the mean, variance, and prior of each class, were written as constants in the ESP32 program. The classification function computes Equations (2) and (3) locally every 10 seconds. This embedded machine learning approach allows classification to continue when the internet connection is lost, provides low latency, and requires no paid server.

3. Results and Discussion

3.1 Implementation and Sensor Calibration

The system was successfully installed and operated in the Cocotani Hydroponic greenhouse. The calibration results in Table 3 show that the reading differences of all sensors were well below the tolerance limits. The DHT22 differed by only 0.2–0.3 °C for temperature and 0.5–0.7% for humidity across four test conditions spanning 26.1–38.5 °C. After correction, the pH sensor differed by 0.01–0.06 pH and the TDS sensor by 1–13 ppm, or less than 1.2% of the reference value. Thus, the data produced are suitable for modeling.

Table 3. Summary of Sensor Calibration Results

Sensor	Number of tests	Difference	Tolerance	Status
DHT22 (temperature)	4	0.2–0.3 °C	±0.5 °C	Valid
DHT22 (humidity)	4	0.5–0.7% RH	±5% RH	Valid
pH PH-4502C	4	0.01–0.06 pH	±0.2 pH	Valid
TDS Meter V1.0	3	1–13 ppm	±10%	Valid

3.2 Environmental Patterns over 31 Days

Figure 3 shows a consistent diurnal pattern throughout the observation period. Air temperature rose during the day to a maximum of 45.1 °C and fell at night to a minimum of 23.9 °C, whereas humidity showed the opposite pattern, with the highest value of 100% at night and the lowest of 48.5% during the day. This pattern is consistent with the tropical climate of Makassar and a greenhouse without climate control.

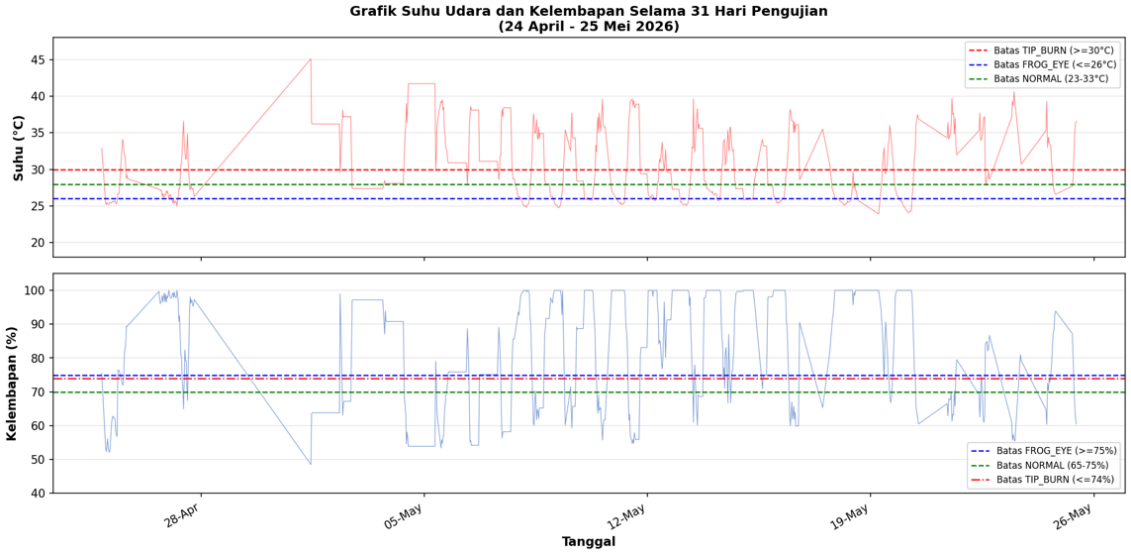


Figure 3. Air Temperature and Relative Humidity over the 31-Day Observation Period

The data distribution in the temperature–humidity feature space is shown in Figure 4. The three classes occupy distinct regions along the inverse relationship between temperature and humidity, with the NORMAL class lying in the transition zone between the two risk classes. Some FROG_EYE data lie at temperatures of approximately 26–29 °C, slightly above the literature range in Table 1, which is also reflected in the mean temperature of this class in the real-data model. The class distribution in Table 2 shows the dominance of FROG_EYE (56.72%) because the humid night period is longer, followed by TIP_BURN (29.35%) during the day, whereas NORMAL (13.93%) appears only during the morning and evening transition hours.

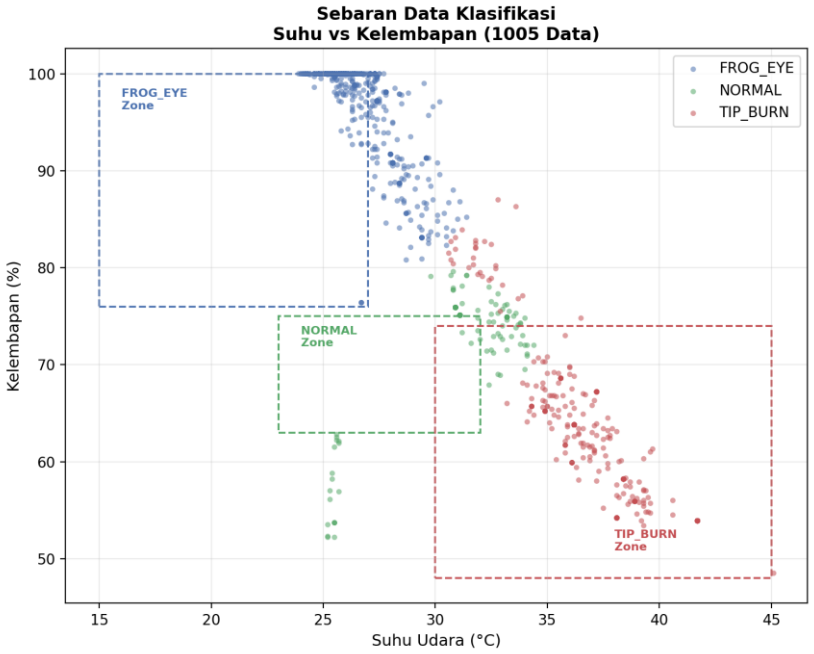


Figure 4. Data Distribution by Air Temperature and Relative Humidity

3.3 Performance of the Simulation and Real-Data Models

The simulation model achieved 95.56% accuracy on 90 test samples, with cross-validation accuracy of 95.56–96.44% across the four methods. This result verifies that the class condition parameters in Table 1 are probabilistically separable. However, because the simulated data are synthetic, balanced, and noise-free, the simulation model serves only as a baseline and is not used in the operational system.

The real-data model was trained offline on 804 field samples as a candidate parameter update for the ESP32. The model parameters in Table 4 show a clear separation of distribution centers: FROG_EYE at lower temperature with very high humidity, TIP_BURN at high temperature with low humidity, and NORMAL between the two. The prior values follow the class proportions of the training data.

Table 4. Parameters of the Real-Data Model

Class	μ temperature (°C)	σ² temperature	μ humidity (%)	σ² humidity	Prior
FROG_EYE	27.1159	2.1965	95.5229	30.0531	0.5144
NORMAL	30.8486	6.6364	71.9524	47.9831	0.1589
TIP_BURN	36.7977	6.5987	63.4389	56.4261	0.3268

The confusion matrix in Figure 5 shows that 189 of the 201 test samples were correctly classified, giving an accuracy of 94.03% with respect to the model-generated labels. All

NORMAL samples were correctly classified (28/28), 109 of 114 FROG_EYE samples were correct, and 52 of 59 TIP_BURN samples were correct. All 12 errors fell into the NORMAL class, and no FROG_EYE sample was confused with TIP_BURN or vice versa. This pattern is reasonable because the NORMAL class lies in the transition zone bordering both risk classes.

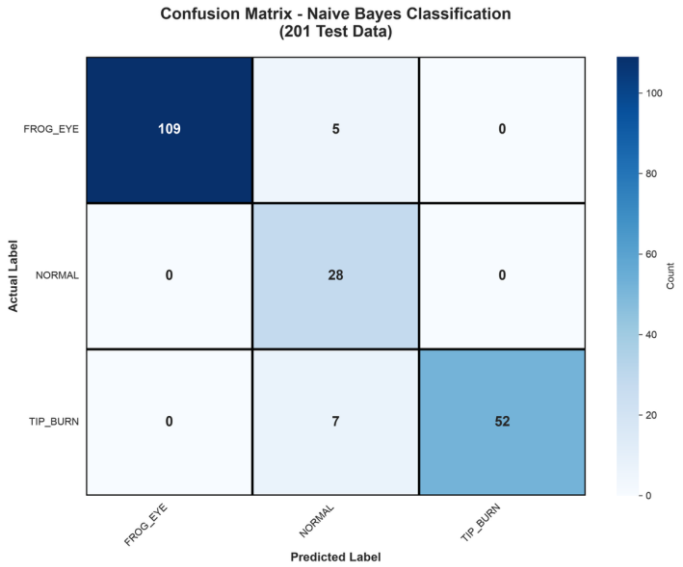


Figure 5. Confusion Matrix of the Real-Data Model on 201 Test Samples

Table 5 summarizes the per-class metrics. The FROG_EYE and TIP_BURN classes achieved a precision of 1.0000, meaning that every risk-class alert issued by the model matched the test data label. The NORMAL class had the lowest precision (0.7000) and an F1-score of 0.8235 because it received all misclassifications and had the fewest samples. From an early-warning perspective, this pattern means that model errors tend to be missed alerts at zone boundaries rather than false alarms. This statement refers to disagreement with the model-generated labels; against visual observations of plants (Section 3.5), the dominant disagreement was instead a risk alert not accompanied by visible symptoms.

Table 5. Classification Report of the Real-Data Model

Class	Precision	Recall	F1-score	Support
FROG_EYE	1.0000	0.9561	0.9776	114
NORMAL	0.7000	1.0000	0.8235	28
TIP_BURN	1.0000	0.8814	0.9369	59
Macro avg	0.9000	0.9458	0.9127	201
Weighted avg	0.9582	0.9403	0.9442	201

The cross-validation results in Table 6 show high consistency. For the real-data model, the accuracy of the four methods ranged from 92.79% to 92.91%, a spread of only 0.12%. The large LOO standard deviation does not indicate instability but is a consequence of testing one sample per iteration, so that each score is either 0% or 100%. The test accuracy (94.03%) is slightly higher than the mean cross-validation accuracy (92.87%), indicating no overfitting. The 1.53-point decrease in accuracy from the simulation model to the real-data model is also reasonable because field data contain sensor noise and an imbalanced class distribution.

Table 6. Cross-Validation Results of the Simulation and Real-Data Models

Method	Simulation: accuracy (%)	Simulation: std (%)	Real data: accuracy (%)	Real data: std (%)
3-fold CV	96.44	1.37	92.79	0.47
5-fold CV	95.78	1.78	92.91	0.85
10-fold CV	96.00	2.59	92.91	2.37
LOO CV	95.56	20.61	92.91	25.67
Test data	95.56	–	94.03	–

It should be emphasized that, because the labels originate from the output of the literature-based initial model, the above accuracy measures how consistently the real-data model reproduces this environmental condition classification, not its ability to diagnose symptoms on plants. Therefore, agreement with actual plant conditions was evaluated separately through visual validation in Section 3.5.

3.4 Functional Testing of the IoT System

The functional test results in Table 7 show that all features operated as targeted. Over the 31-day observation period, the system recorded 1,005 valid records and sent 1,488 periodic monitoring messages and 47 alert messages without delivery failures. An example of the Telegram notifications is shown in Figure 6. Each report contains the classification result with recommended actions, accompanied by a separate message reporting the pH and TDS status.

Table 7. Functional Test Results of the IoT System

Feature	Target	Result	Status
DHT22 sensor reading	10 s	10 s	Passed
Naive Bayes classification	*Real-time*	*Real-time* (embedded)	Passed
Telegram monitoring report	30 min	30 min	Passed
Blynk update	10 min	10 min	Passed
Google Sheets logging	30 min	30 min	Passed
OLED display	*Real-time*	*Real-time*	Passed

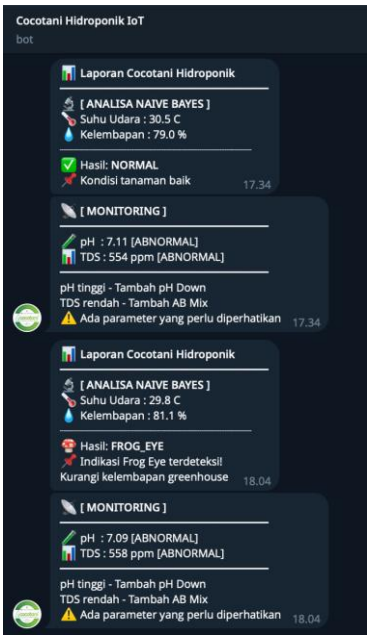


Figure 6. Example of Telegram Notifications for Classification and Monitoring Results

3.5 Field Visual Validation

Visual validation was performed on the classification results of the initial model running on the ESP32. Of the 25 samples, overall agreement reached 52% (13 of 25 samples), as summarized in Table 8. The TIP_BURN class agreed in 13 of 23 samples (56.52%), whereas both FROG_EYE samples disagreed. The very small number of FROG_EYE samples means that this figure cannot yet be generalized.

Table 8. Summary of Model Results against Visual Observations

Model output	Number of samples	Agreed	Agreement (%)
TIP_BURN	23	13	56.52
FROG_EYE	2	0	0.00
Total	25	13	52.00

Most disagreements occurred in the morning at around 07:40–08:35 and in the afternoon approaching 18:00, when the temperature was 28–31 °C and humidity was 61–64%, that is, near the boundary between the TIP_BURN and NORMAL classes. This finding indicates that momentarily detected risky environmental conditions are not always accompanied by visible symptoms, because tissue damage due to calcium deficiency or fungal infection develops cumulatively and requires exposure over a certain duration (de Bang et al., 2021; Mirah et al., 2023). Thus, the system is valid as an early warning of conditions conducive to tip burn and frog eye, but it cannot be claimed to be a direct symptom diagnosis tool.

3.6 Comparison with Previous Studies

Table 9 compares this study with related studies by ground-truth type and inference location. Accuracy values are not compared because the studies use different datasets, target classes, and ground truth, so they are not directly comparable; in this study, the 94.03% figure measures agreement with model-generated labels. The main distinguishing feature of this study is on-device classification of environmental risk for tip burn and frog eye based on real-time sensor data, without requiring images, external servers, or symptom input from users.

Table 9. Comparison with Previous Studies

Study	Method and data	Ground truth	Inference location
Hamidon and Ahamed (2022)	CNN, leaf images	Manual bounding-box labels (LabelImg)	Computer/server
Meshram et al. (2022)	*Naive Bayes, symptom data*	Symptom-disease records (human diseases)	Python server
Saputra and Santiyasa (2024)	*Naive Bayes, soil and air sensors*	Rule-based watering labels from literature ranges; manual check	ESP32 and server
Susanto et al. (2026)	*Naive Bayes, symptom input*	Expert assessment	Web application
This study	*Gaussian Naive Bayes, temperature and humidity*	Labels from initial model; 25 visually validated alerts	ESP32 (initial model); Python (real-data model, offline)

The limitations of this study include the small amount of NORMAL class data, which lowers its precision; static model parameters, so that updates require re-uploading the firmware; the dependence of notification delivery on Wi-Fi connectivity; an analog pH sensor prone to drift; the absence of an independent, expert-labelled ground truth, because all labels were generated by the initial model; and the still limited number of visual validation samples, all drawn from issued alerts, which prevents estimating missed detections.

4. Conclusions

This study successfully developed an early detection system for tip burn and frog eye risk in hydroponic lettuce that integrates DHT22, pH, and TDS sensors with Gaussian Naive Bayes classification running directly on the ESP32 (initial model) and Telegram notifications. Using only two features, air temperature and relative humidity, the real-data model consistently reproduced the environmental condition classification on field data without ever confusing the two risk classes, and its performance was stable across various cross-validation schemes. Visual validation showed that momentarily detected risk conditions are not necessarily followed by visible symptoms; hence, the main value of the system lies in its ability to provide warnings before symptoms develop rather than in diagnosis. Future research should add detection based on accumulated exposure duration, increase NORMAL class data through greenhouse climate control, expand the number of visual validation samples, particularly for frog eye, update the ESP32 parameters with the real-data model after further validation, and compare Naive Bayes with other algorithms such as Random Forest, SVM, and KNN on the same dataset.

Acknowledgements

[Optional — acknowledge the institutions that provided financial support for this research, or delete this section.]

References

Ali, A., Hussain, T., Tantashutikun, N., Hussain, N., & Cocetta, G. (2023). Application of smart techniques, Internet of Things and data mining for resource use efficient and sustainable crop production. *Agriculture, 13*(2), 397. https://doi.org/10.3390/agriculture13020397

de Bang, T. C., Husted, S., Laursen, K. H., Persson, D. P., & Schjoerring, J. K. (2021). The molecular–physiological functions of mineral macronutrients and their consequences for deficiency symptoms in plants. *New Phytologist, 229*(5), 2446–2469. https://doi.org/10.1111/nph.17074

Dolatabadian, A., Neik, T. X., Danilevicz, M. F., Upadhyaya, S. R., Batley, J., & Edwards, D. (2025). Image-based crop disease detection using machine learning. *Plant Pathology, 74*(1), 18–38. https://doi.org/10.1111/ppa.14006

Flores-Iwasaki, M., Guadalupe, G. A., Pachas-Caycho, M., Chapa-Gonza, S., Mori-Zabarburú, R. C., & Guerrero-Abad, J. C. (2025). Internet of Things (IoT) sensors for water quality monitoring in aquaculture systems: A systematic review and bibliometric analysis. *AgriEngineering, 7*(3), 78. https://doi.org/10.3390/agriengineering7030078

Gourshettiwar, P., & Reddy, K. T. V. (2026). IoT-based smart hydroponic system for nutrient management using predictive machine learning algorithms. *Journal of Computer Science, 22*(3), 960–980. https://doi.org/10.3844/jcssp.2026.960.980

Hamidon, M. H., & Ahamed, T. (2022). Detection of tip-burn stress on lettuce grown in an indoor environment using deep learning algorithms. *Sensors, 22*(19), 7251. https://doi.org/10.3390/s22197251

Harjanto, A., Nugroho, H., Ainurrosyidah, A. A., & Burhandenny, A. E. (2026). Improving TDS sensor accuracy in an IoT-based fertigation prototype using polynomial regression calibration and interpolation. *International Journal of Engineering, Science and Information Technology, 6*(1), 36–43. https://doi.org/10.52088/ijesty.v6i1.1776

Kurniawan, R. T., & Putra, M. Y. (2026). Implementasi sistem irigasi hidroponik berbasis Internet of Things di Kampung Ramah Lingkungan [Implementation of an IoT-based hydroponic irrigation system in an eco-friendly village]. *CHAIN: Journal of Computer Technology, Computer Engineering and Informatics, 4*(4), 554–566. https://doi.org/10.58602/chain.v4i4.387

Lestari, I. A., Rahayu, A., & Mulyaningsih, Y. (2022). Pertumbuhan dan produksi tanaman selada (*Lactuca sativa* L.) pada berbagai media tanam dan konsentrasi nutrisi pada sistem hidroponik nutrient film technique (NFT) [Growth and production of lettuce on various growing media and nutrient concentrations in an NFT hydroponic system]. *Jurnal*

Agronida, 8(1), 31–39.

Luo, J., Li, B., & Leung, C. (2024). A survey of computer vision technologies in urban and controlled-environment agriculture. *ACM Computing Surveys, 56*(5). https://doi.org/10.1145/3626186

Meshram, S., Dongre, S., & Fole, T. (2022). Disease prediction system using naïve Bayes. *International Journal for Research in Applied Science and Engineering Technology, 10*(12), 1492–1496. https://doi.org/10.22214/ijraset.2022.48002

Mirah, A. A. I., Darmadi, A. A. K., Suriani, N. L., & Swantara, M. D. (2023). *Cercospora canescens*: Cause of leaf spot disease on lettuce crop in Bali Province, Indonesia. *SABRAO Journal of Breeding and Genetics, 55*(6), 2006–2016. https://doi.org/10.54910/sabrao2023.55.6.14

Mohyuddin, G., Khan, M. A., Haseeb, A., Mahpara, S., Waseem, M., & Saleh, A. M. (2024). Evaluation of machine learning approaches for precision farming in smart agriculture system: A comprehensive review. *IEEE Access, 12*, 60155–60184. https://doi.org/10.1109/ACCESS.2024.3390581

Nguanhom, J., Cheewangkoon, R., Groenewald, J. Z., Braun, U., To-Anan, C., & Crous, P. W. (2015). Taxonomy and phylogeny of *Cercospora* spp. from Northern Thailand. *Phytotaxa, 233*(1), 27–48. https://doi.org/10.11646/phytotaxa.233.1.2

Prabowo, M. C. A., Janitra, A. A., & Wibowo, N. M. (2023). Sistem monitoring hidroponik berbasis IoT dengan sensor suhu, pH, dan ketinggian air menggunakan ESP8266 [IoT-based hydroponic monitoring system with temperature, pH, and water level sensors using ESP8266]. *Jurnal Tecnoscienza, 7*(2), 312–323. https://doi.org/10.51158/tecnoscienza.v7i2.894

Prasetyo, A., Nugroho, A. B., & Setyawan, H. (2022). Perancangan sistem monitoring pada hidroponik selada (*Lactuca sativa* L.) dengan metode NFT berbasis Internet of Things (IoT) [Design of an IoT-based monitoring system for NFT hydroponic lettuce]. *Jurnal Teknik Elektro dan Komputasi (ELKOM), 4*(2), 99–109. https://doi.org/10.32528/elkom.v4i2.6102

Purwalaksana, A. Z., Khan, S. R., Saputra, A. F. S., Akmalluddin, M., Wahyu, S., & Rismawati, E. (2024). Penerapan sistem hidroponik berbasis sensor untuk pemberdayaan Desa Majalaya [Application of a sensor-based hydroponic system for the empowerment of Majalaya Village]. *Jurnal Pengabdian Masyarakat Sains dan Aplikasinya (JPMSA), 4*(2), 14–19. https://doi.org/10.21009/jpmsa.v4i2.49491

Qin, Y. M., Tu, Y. H., Li, T., Ni, Y., Wang, R. F., & Wang, H. (2025). Deep learning for sustainable agriculture: A systematic review on applications in lettuce cultivation. *Sustainability, 17*(7), 3190. https://doi.org/10.3390/su17073190

Riansyah, A., Mustafa, & Syakhroni, A. (2025). Penerapan teknologi IoT pada hidroponik di sekolah dasar untuk meningkatkan literasi sains dan kesadaran lingkungan [Application of IoT technology in elementary school hydroponics to improve science literacy and environmental awareness]. *Abdimas Universal, 7*(2), 321–326. https://doi.org/10.36277/abdimasuniversal.v7i2.2681

Saputra, M. Y., & Santiyasa, I. W. (2024). Optimizing machine learning performance with the naive Bayes classifier process in smart farming. *Jurnal Nasional Pendidikan Teknik Informatika (JANAPATI), 13*(2), 382–393. https://doi.org/10.23887/janapati.v13i2.76926

Shafik, W., Tufail, A., Namoun, A., De Silva, L. C., & Apong, R. A. A. H. M. (2023). A systematic literature review on plant disease detection: Motivations, classification techniques, datasets, challenges, and future trends. *IEEE Access, 11*, 59174–59203. https://doi.org/10.1109/ACCESS.2023.3284760

Supakitthanakorn, S., Ruangwong, O. U., & Boonyawan, D. (2023). Inactivation of *Cercospora lactucae-sativa* through application of non-thermal atmospheric pressure gliding arc, tesla coil and dielectric barrier discharge plasmas. *Applied Sciences, 13*(11), 6643. https://doi.org/10.3390/app13116643

Susanto, E. S., Aldy, Esabella, S., & Ekastini. (2026). Implementasi sistem pakar berbasis web untuk diagnosis penyakit tanaman padi menggunakan metode naive Bayes di Balai Penyuluh Pertanian Kecamatan Moyo Hulu [Implementation of a web-based expert system for rice disease diagnosis using the naive Bayes method at the Moyo Hulu agricultural extension center]. *JTK3TI: Jurnal Tata Kelola dan Kerangka Kerja TI, 12*(1), 122–130.

Syaimah, S. N., Zulfarosda, R., Purnamasari, R. T., & Arifin, A. Z. (2025). Analisis pertumbuhan dan hasil tanaman selada (*Lactuca sativa* L.) hidroponik dengan perbedaan temperatur air [Analysis of growth and yield of hydroponic lettuce under different water temperatures]. *Ziraa'ah, 50*(2), 327–339.

Tarigan, F., Buaton, R., & Ramadani, S. (2023). IoT-based hydroponic plant monitoring system. *Journal of Artificial Intelligence and Engineering Applications*. https://ioinformatic.org/

To-Anun, C., & Meeboon, J. (2011). *Genus Cercospora in Thailand: Taxonomy and phylogeny (with a dichotomous key to species)*.

Valleggi, L., & Stefanini, F. M. (2024). A mini-review on data science approaches in crop yield and disease detection. *Frontiers in Agronomy, 6*, 1352219. https://doi.org/10.3389/fagro.2024.1352219

Wati, D. R., & Sholihah, W. (2021). Pengontrol pH dan nutrisi tanaman selada pada hidroponik sistem NFT berbasis Arduino [Arduino-based pH and nutrient controller for lettuce in an NFT hydroponic system]. *Multinetics, 7*(1), 12–20.

Zahra, N., Muthiadin, C., & Ferial. (2023). Budidaya tanaman selada (*Lactuca sativa* L.) secara hidroponik dengan sistem DFT di BBPP Batangkaluku [Hydroponic cultivation of lettuce using the DFT system at BBPP Batangkaluku]. *Filogeni: Jurnal Mahasiswa Biologi, 3*(1), 18–22. https://doi.org/10.24252/filogeni.v3i1.29922